

¹ gdess: A framework for evaluating simulated atmospheric CO₂ in Earth System Models

³ **Daniel E. Kaufman¹, Sha Feng², Katherine V. Calvin¹, Bryce E.
⁴ Harrop², and Susannah M. Burrows²**

⁵ **1** Joint Global Change Research Institute, Pacific Northwest National Laboratory, College Park, MD,
⁶ **2** Atmospheric Sciences and Global Change Division, Pacific Northwest National Laboratory,
⁷ Richland, WA, USA

DOI: [10.xxxxxx/draft](https://doi.org/10.xxxxxx/draft)

Software

- [Review ↗](#)
- [Repository ↗](#)
- [Archive ↗](#)

Editor: David Hagan [↗](#)

Reviewers:

- [@slayoo](#)
- [@sr ridge](#)
- [@simonom](#)

Submitted: 03 September 2021

Published: unpublished

License

Authors of papers retain
copyright and release the work
under a Creative Commons
Attribution 4.0 International
License ([CC BY 4.0](#)).

⁸ Summary

⁹ Atmospheric carbon dioxide (CO₂) plays a key role in the global carbon cycle and global
¹⁰ warming. Climate-carbon feedbacks are often studied and estimated using Earth System
¹¹ Models (ESMs), which couple together multiple model components—including the atmosphere,
¹² ocean, terrestrial biosphere, and cryosphere—to jointly simulate mass and energy exchanges
¹³ within and between these components. Despite tremendous advances, model intercomparisons
¹⁴ and benchmarking are aspects of ESMs that warrant further improvement (Fer et al., 2021;
¹⁵ Smith et al., 2014). Such benchmarking is critical because comparing the value of state variables
¹⁶ in these simulations against observed values provides evidence for appropriately refining model
¹⁷ components; moreover, researchers can learn much about Earth system dynamics in the process
¹⁸ (Randall et al., 2019).

¹⁹ We introduce gdess (a.k.a., Greenhouse gas Diagnostics for Earth System Simulations), which
²⁰ parses observational datasets and ESM simulation output, combines them to be in a consistent
²¹ structure, computes statistical metrics, and generates diagnostic visualizations. In its current
²² incarnation, gdess facilitates evaluating a model's ability to reproduce observed temporal
²³ and spatial variations of atmospheric CO₂. The diagnostics implemented modularly in gdess
²⁴ support more rapid assessment and improvement of model-simulated global CO₂ sources and
²⁵ sinks associated with land and ocean ecosystem processes. We intend for this set of automated
²⁶ diagnostics to form an extensible, open source framework for future comparisons of simulated
²⁷ and observed concentrations of various greenhouse gases across Earth system models.

²⁸ Statement of need

²⁹ Thorough evaluation of simulated atmospheric CO₂ concentrations—by comparing against
³⁰ observations—requires multiple diagnostics, metrics, and visualizations. During the past
³¹ decade, such evaluations have utilized certain common methods, such as aggregating in situ
³² measurements into latitude bands and detrending of multidecadal time series to investigate
³³ seasonal cycles (Chevallier et al., 2019; Jing et al., 2018; Keppel-Aleks et al., 2013; Liptak et
³⁴ al., 2017; Ott et al., 2015; Weir et al., 2021). However, the construction of diagnostics used
³⁵ in these evaluations has not been automated in an open-source tool available to the broader
³⁶ atmospheric modeling community. Thus, each modeling or analysis team has had to decide
³⁷ on and code their own preferred set of diagnostics, resulting in redundancies and potential
³⁸ inconsistencies among efforts.

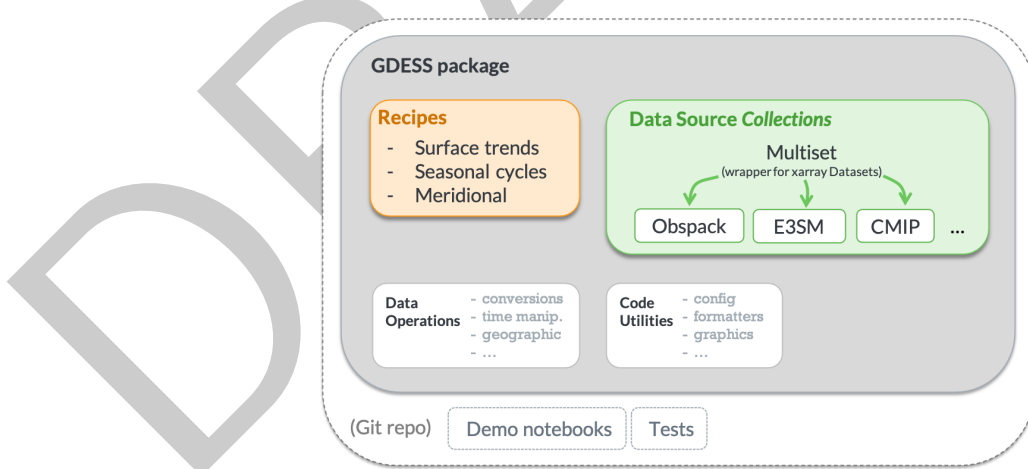
³⁹ Several software packages have been developed to streamline the application of diagnostics for
⁴⁰ ESM benchmarking. These tools share related functionality with gdess, and some have directly
⁴¹ inspired the gdess design and our development approach. For example, the ESM Evaluation

42 Tool (ESMValTool; Eyring, Righi, et al. (2016); Eyring et al. (2020)) has been used to
 43 generate specific figures from the literature—including a comparison of column-averaged CO₂
 44 values as performed by Gier et al. (2020)—but does not provide for tailored processing of varied
 45 CO₂ data sources. We adopted the term *recipe* from its use by ESMValTool. The International
 46 Land Model Benchmarking (ILAMB) System (Collier et al., 2018) excels at intercomparisons
 47 between multiple land models and has been used to benchmark inferred CO₂ concentrations
 48 against surface station measurements (Wu et al., 2020). In contrast to gdess, ILAMB provides
 49 the means to evaluate emulated results but not prognostic simulations for CO₂ (Keppel-Aleks,
 50 2021).

51 Design and data sources

52 gdess is written in Python [“version 3”; Python Core Team (2015); Van Rossum & Drake
 53 (2009)]. A comprehensive readme file and docstrings throughout the open source codebase
 54 (<https://github.com/E3SM-Project/gdless>) provide documentation and guidance, and Continuous
 55 Integration tests facilitate further code development and maintenance. Data variables are
 56 represented and handled in memory using xarray, an open-source Python package for working
 57 with labeled multi-dimensional arrays (Hoyer & Hamman, 2017).

58 As shown in Figure 1, gdess is organized into modular components. A *Collection* class
 59 encapsulates source-specific attributes and methods for each data source (described below)
 60 and each Collection inherits common attributes from a parent *Multiset* class. Each diagnostic
 61 recipe, defined in a separate module file (e.g., `surface_trends.py`), instantiates and uses
 62 Collection objects to handle the loading and pre-processing of data. Additionally, visualization
 63 functions (e.g., time-series, annual cycles) are accessible from any instance of a Collection or
 64 Multiset so that data sources can be inspected individually—i.e., without the need to run one
 65 of the comparative diagnostic recipes.



66 **Figure 1:** Schematic of the gdess code structure.

67 gdess can process data from three sources: Globalview+, CMIP, and E3SM. Data from surface
 68 observing stations must be retrieved from the NOAA Global Monitoring Laboratory (GML)
 69 Globalview+ version 6.0 Observation package (Obspack; Schuldt et al. (2020); Masarie et al.
 70 (2014)). In situ and flask measurements can be used from approximately 200 stations whose
 data in Obspack spans at least a 12 month period (Figure 2).

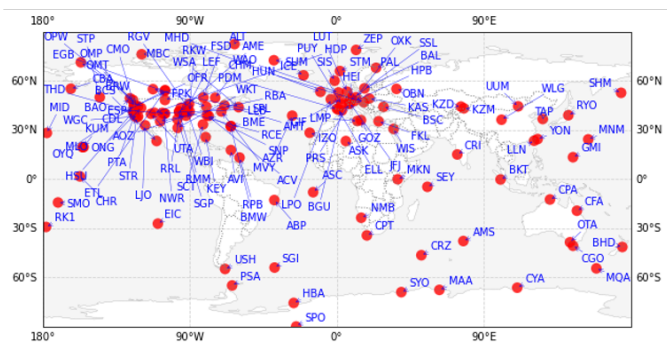


Figure 2: Global map showing surface observing station locations (red circles) and their three-letter site codes, as recorded in Obspack and used in gdesc.

We distinguish between the model results from two different sources: (i) simulations by the Energy Exascale Earth System Model (E3SM), and (ii) other Earth system models participating in the latest, Version 6, Coupled Model Intercomparison Project (CMIP6). E3SM is a global modeling system composed of multiple coupled subcomponent models: atmosphere, ocean, land, ice ([Burrows et al., 2020](#); [Golaz et al., 2019](#)). In this study, our focus is on evaluating CO₂ mole fractions in the atmospheric component, which is called the E3SM atmosphere model (EAM) and which has been described in detail by Rasch et al. ([2019](#)).

CMIP6 organizes the setup, experimental design, and intercomparisons of simulations performed using numerous global climate models. Data from CMIP6 are accessed either via locally stored files—downloaded directly from Earth System Grid Federation (ESGF) data nodes—or programmatically via the *intake-esm* package, which is a gdess dependency maintained as part of the *Pangeo* project. By default, comparisons in gdess use data from the ‘esm-hist’ experiment, which contains CO₂ emission-driven simulations that span the period of 1850 to 2014—i.e., an “all-forcing simulation of the recent past with atmospheric CO₂ concentration calculated” ([Eyring, Bony, et al., 2016](#)). We expect model output from any CMIP6 experiment could be used by specifying the appropriate data identifier or file location, although additional testing would be needed to confirm expected behavior.

Functionality

This section describes and provides example output from the three diagnostic recipes implemented in gess. These recipes can be initiated either from a terminal or from within a running Python kernel. The command-line interface consists of the gess command, followed by the type of recipe, and then options for each recipe—e.g., which observing station(s) to use for comparison. Within a Python kernel, options are specified via a dictionary object.

94 Multidecadal trend

95 Skillful simulation of the historical multidecadal trend in atmospheric CO₂ is a necessary
96 condition for an ESM to be an effective tool for conducting climatological projections and
97 analyses. The research questions one might address with this diagnostic recipe (see example
98 output in Figure 3) include: What are the long-term biases in the model simulation? How
99 does the simulated increase in CO₂ mixing ratios compare to surface measurements?

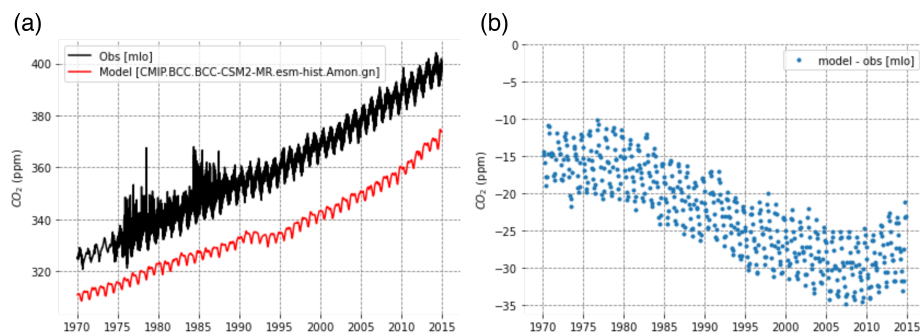


Figure 3: Example output of the `surface_trends` recipe, showing (a) individual time series and (b) differences between simulated and observed concentrations of surface-level atmospheric CO₂ at the Mauna Loa Observatory, Hawaii (MLO).

100 Seasonal cycle

101 Because of the substantial impact primary production and respiration have on CO₂ concentrations,
 102 evaluating the seasonal cycle at a given location can help disentangle the effects of
 103 biological from physical processes. The seasonal cycle can be quantified by “the projection of
 104 an atmospheric time series onto a suitably defined subset of orthogonal basis functions, the
 105 choice of which depends on the length of the series involved” (Straus, 1983). For computing
 106 the seasonal cycle, we detrend the time series by fitting a function composed of both polynomial
 107 and harmonic terms, following the procedure of Sweeney et al. (2015) and originally proposed
 108 by Thoning & Tans (1989). Example output of the `seasonal_cycle` recipe is shown in Figure 4.

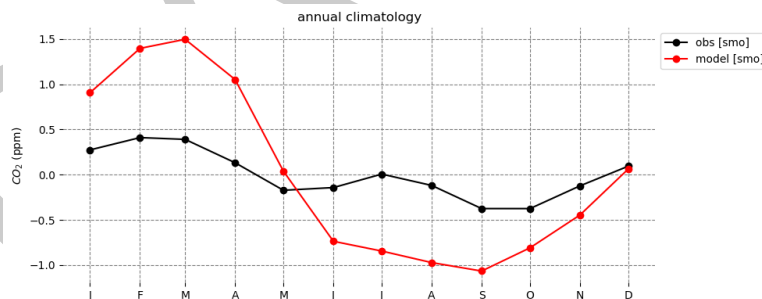


Figure 4: Example output of the `seasonal_cycle` recipe, comparing annual climatologies of surface atmospheric CO₂ concentrations at the American Samoa Observatory, Tutuila Island (SMO).

109 Meridional gradient

110 By comparing CO₂ concentrations across observing sites distributed globally, we can assess
 111 whether simulated transport and mixing is skillfully reproducing spatial gradients. For instance,
 112 the surface CO₂ flux signals at lower latitudes (30–45°N) are moved to northern boreal latitudes
 113 and also to the south by large scale circulation. Spatial analysis can reveal evidence of southward
 114 movement toward (sub)tropical convection that becomes mixed with Hadley circulation or
 115 northward movement toward midlatitude synoptic weather patterns and the Ferrell circulation
 116 (Denning et al., 1999; Schuh et al., 2019; Stephens et al., 2007). Figure 5 shows example
 117 output of the `meridional` recipe.

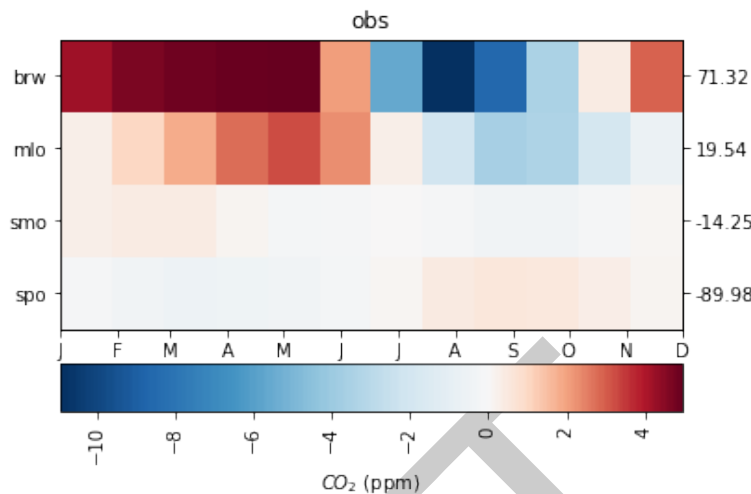


Figure 5: Example output of the meridional recipe, comparing the seasonal cycle across latitudes, at locations of user-specified surface stations.

118 Outlook

119 Currently, gdess is helping to assess simulations using the biogeochemistry configuration
 120 of E3SM, with the aim of exploring carbon-climate interactions. In addition to the three
 121 implemented recipes (multidecadal trends, seasonal cycles, and meridional gradients), current
 122 development includes two other methods—by which CO₂ was also evaluated by Keppel-Aleks
 123 et al. (2013)—vertical gradients and interannual variability. Future releases may evaluate
 124 vertical gradients using aircraft data from Globalview+ Obspack, include satellite data, and
 125 extend to data for other greenhouse gases, such as methane.

126 Acknowledgements

127 We thank Drs. Colm Sweeney and Kirk Thoning, at the NOAA Global Monitoring Laboratory,
 128 for providing code and support for implementing the curve fitting methods. A dataset file
 129 provided via the Obspack from the Mauna Loa surface observing station is included in the tests
 130 directory with permission from the data provider, Keeling et al. (2001). This research was
 131 supported as part of the Energy Exascale Earth System Model (E3SM) project, funded by the
 132 U.S. Department of Energy (DOE), Office of Science, Office of Biological and Environmental
 133 Research. Data analysis described in this work relied on computational resources provided
 134 by the National Energy Research Scientific Computing Center, a DOE Office of Science User
 135 Facility supported by the Office of Science of the U.S. Department of Energy under Contract
 136 DE-AC02-05CH11231. The Pacific Northwest National Laboratory (PNNL) is operated for
 137 DOE by Battelle Memorial Institute under Contract DE-AC05-76RLO1830.

138 References

- 139 Burrows, S. M., Maltrud, M., Yang, X., Zhu, Q., Jeffery, N., Shi, X., Ricciuto, D., Wang,
 140 S., Bisht, G., Tang, J., Wolfe, J., Harrop, B. E., Singh, B., Brent, L., Baldwin, S.,
 141 Zhou, T., Cameron-Smith, P., Keen, N., Collier, N., ... Leung, L. R. (2020). The DOE
 142 E3SM v1.1 Biogeochemistry Configuration: Description and Simulated Ecosystem-Climate
 143 Responses to Historical Changes in Forcing. *J. Adv. Model. Earth Syst.*, 12(9), 1–59.
 144 <https://doi.org/10.1029/2019MS001766>

- 145 Chevallier, F., Remaud, M., O'Dell, C. W., Baker, D., Peylin, P., & Cozic, A. (2019). Objective
 146 evaluation of surface- and satellite-driven carbon dioxide atmospheric inversions. *Atmos.*
 147 *Chem. Phys.*, 19(22), 14233–14251. <https://doi.org/10.5194/acp-19-14233-2019>
- 148 Collier, N., Hoffman, F. M., Lawrence, D. M., Keppel-Aleks, G., Koven, C. D., Riley, W.
 149 J., Mu, M., & Randerson, J. T. (2018). The International Land Model Benchmarking
 150 (ILAMB) System: Design, Theory, and Implementation. *J. Adv. Model. Earth Syst.*,
 151 10(11), 2731–2754. <https://doi.org/10.1029/2018MS001354>
- 152 Denning, A. S., Holzer, M., Gurney, K. R., Heimann, M., Law, R. M., Rayner, P. J., Fung,
 153 I. Y., Fan, S.-M., Taguchi, S., Friedlingstein, P., Balkanski, Y., Taylor, J., Maiss, M.,
 154 & Levin, I. (1999). Three-dimensional transport and concentration of SF₆ A model
 155 intercomparison study (TransCom 2). *Tellus B: Chemical and Physical Meteorology*, 51(2),
 156 266–297. <https://doi.org/10.3402/tellusb.v51i2.16286>
- 157 Eyring, V., Bock, L., Lauer, A., Righi, M., Schlund, M., Andela, B., Arnone, E., Bellprat, O.,
 158 Carvalhais, N., Cionni, I., Cortesi, N., Crezee, B., L. Davin, E., Davini, P., Debeire, K., De
 159 Mora, L., Deser, C., Docquier, D., Earnshaw, P., ... Zimmermann, K. (2020). Earth System
 160 Model Evaluation Tool (ESMValTool) v2.0 - An extended set of large-scale diagnostics for
 161 quasi-operational and comprehensive evaluation of Earth system models in CMIP. *Geosci.*
 162 *Model Dev.*, 13(7), 3383–3438. <https://doi.org/10.5194/gmd-13-3383-2020>
- 163 Eyring, V., Bony, S., Meehl, G. A., Senior, C. A., Stevens, B., Stouffer, R. J., & Taylor, K.
 164 E. (2016). Overview of the Coupled Model Intercomparison Project Phase 6 (CMIP6)
 165 experimental design and organization. *Geosci. Model Dev.*, 9(5), 1937–1958. <https://doi.org/10.5194/gmd-9-1937-2016>
- 166 Eyring, V., Righi, M., Lauer, A., Evaldsson, M., Wenzel, S., Jones, C., Anav, A., Andrews,
 167 O., Cionni, I., Davin, E. L., Deser, C., Ehbrecht, C., Friedlingstein, P., Gleckler, P.,
 168 Gottschaldt, K. D., Hagemann, S., Juckes, M., Kindermann, S., Krasting, J., ... Williams, K.
 169 D. (2016). ESMValTool (v1.0)-a community diagnostic and performance metrics tool for
 170 routine evaluation of Earth system models in CMIP. *Geosci. Model Dev.*, 9(5), 1747–1802.
 171 <https://doi.org/10.5194/gmd-9-1747-2016>
- 172 Fer, I., Gardella, A. K., Shiklomanov, A. N., Campbell, E. E., Cowdery, E. M., De Kauwe, M.
 173 G., Desai, A., Duveneck, M. J., Fisher, J. B., Haynes, K. D., Hoffman, F. M., Johnston,
 174 M. R., Kooper, R., LeBauer, D. S., Mantooth, J., Parton, W. J., Poulter, B., Quaife, T.,
 175 Raiho, A., ... Dietze, M. C. (2021). Beyond ecosystem modeling: A roadmap to community
 176 cyberinfrastructure for ecological data-model integration. *Global Change Biology*, 27(1),
 177 13–26. <https://doi.org/10.1111/gcb.15409>
- 178 Golaz, J.-C., Caldwell, P. M., Van Roekel, L. P., Petersen, M. R., Tang, Q., Wolfe, J. D.,
 179 Abeshu, G., Ananthraj, V., Asay-Davis, X. S., Bader, D. C., Baldwin, S. A., Bisht,
 180 G., Bogenschutz, P. A., Branstetter, M., Brunke, M. A., Brus, S. R., Burrows, S. M.,
 181 Cameron-Smith, P. J., Donahue, A. S., ... Zhu, Q. (2019). The DOE E3SM Coupled
 182 Model Version 1: Overview and Evaluation at Standard Resolution. *Journal of Advances*
 183 *in Modeling Earth Systems*, 11(7), 2089–2129. <https://doi.org/10.1029/2018MS001603>
- 184 Hoyer, S., & Hamman, J. (2017). xarray: N-D labeled arrays and datasets in Python. *Journal*
 185 *of Open Research Software*, 5(1). <https://doi.org/10.5334/jors.148>
- 186 Jing, Y., Wang, T., Zhang, P., Chen, L., Xu, N., & Ma, Y. (2018). Global atmospheric
 187 CO₂ concentrations simulated by GEOS-Chem: Comparison with GOSAT, carbon tracker
 188 and ground-based measurements. *Atmosphere (Basel)*, 9(5). <https://doi.org/10.3390/atmos9050175>
- 189 Keeling, C. D., Piper, S. C., Bacastow, R. B., Wahlen, M., Whorf, T. P., Heimann, M.,
 190 & Meijer, H. A. (2001). *Exchanges of atmospheric CO₂ and ¹³CO₂ with the terrestrial*
 191 *biosphere and oceans from 1978 to 2000. I. Global aspects* (S. D. Scripps Institution

- 194 of Oceanography, Ed.; No. 01-06; p. 88). UC San Diego: Library – Scripps Digital.
195 %7B<https://escholarship.org/uc/item/09v319r9%7D>
- 196 Keppel-Aleks, G. (2021). personal communication.
- 197 Keppel-Aleks, G., Randerson, J. T., Lindsay, K., Stephens, B. B., Keith Moore, J., Doney, S. C.,
198 Thornton, P. E., Mahowald, N. M., Hoffman, F. M., Sweeney, C., Tans, P. P., Wennberg, P.
199 O., & Wofsy, S. C. (2013). Atmospheric carbon dioxide variability in the community earth
200 system model: Evaluation and transient dynamics during the twentieth and twenty-first
201 centuries. *J. Clim.*, 26(13), 4447–4475. <https://doi.org/10.1175/JCLI-D-12-00589.1>
- 202 Liptak, J., Keppel-Aleks, G., & Lindsay, K. (2017). Drivers of multi-century trends in
203 the atmospheric CO₂ mean annual cycle in a prognostic ESM. *Biogeosciences*, 14(6),
204 1383–1401. <https://doi.org/10.5194/bg-14-1383-2017>
- 205 Masarie, K. A., Peters, W., Jacobson, A. R., & Tans, P. P. (2014). ObsPack: A framework for
206 the preparation, delivery, and attribution of atmospheric greenhouse gas measurements.
207 *Earth Syst. Sci. Data*, 6(2), 375–384. <https://doi.org/10.5194/essd-6-375-2014>
- 208 Ott, L. E., Pawson, S., Collatz, G. J., Gregg, W. W., Menemenlis, D., Brix, H., Rousseaux, C.
209 S., Bowman, K. W., Liu, J., Eldering, A., Gunson, M. R., & Kawa, S. R. (2015). Assessing
210 the magnitude of CO₂ flux uncertainty in atmospheric CO₂ records using products from
211 NASA's Carbon Monitoring Flux Pilot Project. *J. Geophys. Res. Atmos.*, 120(2), 734–765.
212 <https://doi.org/10.1002/2014JD022411>
- 213 Python Core Team. (2015). *Python: A dynamic, open source programming language*. Python
214 Software Foundation. %7B<https://www.python.org/>%7D
- 215 Randall, D. A., Bitz, C. M., Danabasoglu, G., Denning, A. S., Gent, P. R., Gettelman,
216 A., Griffies, S. M., Lynch, P., Morrison, H., Pincus, R., & Thuburn, J. (2019). 100
217 Years of Earth System Model Development. *Meteorol. Monogr.*, 59, 12.1–12.66. <https://doi.org/10.1175/amsmonographs-d-18-0018.1>
- 218 Rasch, P. J., Xie, S., Ma, P. L., Lin, W., Wang, H., Tang, Q., Burrows, S. M., Caldwell, P.,
219 Zhang, K., Easter, R. C., Cameron-Smith, P., Singh, B., Wan, H., Golaz, J. C., Harrop,
220 B. E., Roesler, E., Bacmeister, J., Larson, V. E., Evans, K. J., ... Yang, Y. (2019). An
221 Overview of the Atmospheric Component of the Energy Exascale Earth System Model. *J.
222 Adv. Model. Earth Syst.*, 11(8), 2377–2411. <https://doi.org/10.1029/2019MS001629>
- 223 Schuh, A. E., Jacobson, A. R., Basu, S., Weir, B., Baker, D., Bowman, K., Chevallier,
224 F., Crowell, S., Davis, K. J., Deng, F., Denning, S., Feng, L., Jones, D., Liu, J., &
225 Palmer, P. I. (2019). Quantifying the Impact of Atmospheric Transport Uncertainty
226 on CO₂ Surface Flux Estimates. *Global Biogeochemical Cycles*, 33(4), 484–500. <https://doi.org/10.1029/2018GB006086>
- 227 Schuldt, K. N., Mund, J., Luijckx, I. T., Jacobson, A. R., Cox, A., Vermeulen, A., Manning,
228 A., Beyersdorf, A., Manning, A., Karion, A., Hensen, A., Arlyn Andrews, Frumau, A.,
229 Colomb, A., Scheeren, B., Law, B., Baier, B., Munger, B., Paplawsky, B., ... Loh, Z.
230 (2020). *Multi-laboratory compilation of atmospheric carbon dioxide data for the period
231 1957–2019; obspack_co2_1_GLOBALVIEWplus_v6.0_2020-09-11*. NOAA Earth System
232 Research Laboratory, Global Monitoring Division. <https://doi.org/10.25925/20200903>
- 233 Smith, M. J., Palmer, P. I., Purves, D. W., Vanderwel, M. C., Lyutsarev, V., Calderhead,
234 B., Joppa, L. N., Bishop, C. M., & Emmott, S. (2014). Changing How Earth System
235 Modeling is Done to Provide More Useful Information for Decision Making, Science,
236 and Society. *Bulletin of the American Meteorological Society*, 95(9), 1453–1464. <https://doi.org/10.1175/BAMS-D-13-00080.1>
- 237 Stephens, B. B., Gurney, K. R., Tans, P. P., Sweeney, C., Peters, W., Bruhwiler, L., Ciais, P.,
238 Ramonet, M., Bousquet, P., Nakazawa, T., Aoki, S., Machida, T., Inoue, G., Vinnichenko,
239 N., Lloyd, J., Jordan, A., Heimann, M., Shibistova, O., Langenfelds, R. L., ... Denning, A.

- 243 S. (2007). Weak Northern and Strong Tropical Land Carbon Uptake from Vertical Profiles
244 of Atmospheric CO₂. *Science*, 316(5832), 1732–1735. <https://doi.org/10.1126/science.1137004>
- 245
- 246 Straus, D. M. (1983). On the Role of the Seasonal Cycle. *Journal of Atmospheric Sciences*,
247 40(2), 303–313. [https://doi.org/10.1175/1520-0469\(1983\)040%3C0303:OTROTS%3E2.0.CO;2](https://doi.org/10.1175/1520-0469(1983)040%3C0303:OTROTS%3E2.0.CO;2)
- 248
- 249 Sweeney, C., Karion, A., Wolter, S., Newberger, T., Guenther, D., Higgs, J. A., Andrews, A.
250 E., Lang, P. M., Neff, D., Dlugokencky, E., Miller, J. B., Montzka, S. A., Miller, B. R.,
251 Masarie, K. A., Biraud, S. C., Novelli, P. C., Crotwell, M., Crotwell, A. M., Thoning, K.,
252 & Tans, P. P. (2015). Seasonal climatology of CO₂ across North America from aircraft
253 measurements in the NOAA/ESRL Global Greenhouse Gas Reference Network. *J. Geophys.
Res. Atmos.*, 120(10), 5155–5190. <https://doi.org/10.1002/2014JD022591>
- 254
- 255 Thoning, K. W., & Tans, P. P. (1989). Atmospheric carbon dioxide at Mauna Loa Observatory.
256 2. Analysis of the NOAA GMCC data, 1974–1985. *J. Geophys. Res.*, 94(D6), 8549–8565.
257 <https://doi.org/10.1029/JD094iD06p08549>
- 258 Van Rossum, G., & Drake, F. L. (2009). *Python 3 Reference Manual*. CreateSpace.
259 ISBN: 1441412697
- 260 Weir, B., Ott, L. E., Collatz, G. J., Kawa, S. R., Poulter, B., Chatterjee, A., Oda, T., &
261 Pawson, S. (2021). Bias-correcting carbon fluxes derived from land-surface satellite data for
262 retrospective and near-real-time assimilation systems. *Atmospheric Chemistry and Physics*,
263 21(12), 9609–9628. <https://doi.org/10.5194/acp-21-9609-2021>
- 264 Wu, G., Cai, X., Keenan, T. F., Li, S., Luo, X., Fisher, J. B., Cao, R., Li, F., Purdy, A. J.,
265 Zhao, W., Sun, X., & Hu, Z. (2020). Evaluating three evapotranspiration estimates from
266 model of different complexity over China using the ILAMB benchmarking system. *Journal
of Hydrology*, 590, 125553. <https://doi.org/10.1016/j.jhydrol.2020.125553>
- 267